Atmos. Chem. Phys., 15, 1013–1028, 2015
www.atmos-chem-phys.net/15/1013/2015/
doi:10.5194/acp-15-1013-2015


Atmospheric Chemistry and Physics
Open Access

# Correlation slopes of GEM / CO, GEM / $CO_2$, and GEM / $CH_4$ and estimated mercury emissions in China, South Asia, the Indochinese Peninsula, and Central Asia derived from observations in northwestern and southwestern China

**X. W. Fu[1], H. Zhang[1,2], C.-J. Lin[1,3,4], X. B. Feng[1], L. X. Zhou[5], and S. X. Fang[5]**

[1]State Key Laboratory of Environmental Geochemistry, Institute of Geochemistry, Chinese Academy of Sciences, Guiyang 550002, China
[2]Graduate University of the Chinese Academy of Sciences, Beijing 100049, China
[3]Department of Civil Engineering, Lamar University, Beaumont, Texas 77710, USA
[4]College of Energy and Environment, South China University of Technology, Guangzhou 510006, China
[5]Chinese Academy of Meteorological Sciences (CAMS), CMA, Beijing 100081, China

*Correspondence to:* X. B. Feng (fengxinbin@vip.skleg.cn) and L. X. Zhou (zhoulx@cams.cma.gov.cn)

Received: 9 September 2014 – Published in Atmos. Chem. Phys. Discuss.: 30 September 2014
Revised: 15 December 2014 – Accepted: 15 December 2014 – Published: 29 January 2015

**Abstract.** Correlation analyses between atmospheric mercury (Hg) and other trace gases are useful for identification of sources and constraining regional Hg emissions. Emissions of Hg in Asia contribute significantly to the global budget of atmospheric Hg. However, due to the lack of reliable data on the source strength, large uncertainties remain in the emission inventories of Hg in Asia. In the present study, we calculated the correlation slopes of GEM / CO, GEM / $CO_2$, and GEM / $CH_4$ for mainland China, South Asia, the Indochinese Peninsula, and Central Asia using the ground-based observations at three remote sites in northwestern and southwestern China, and applied these values to estimate GEM emissions in the four source regions. The geometric mean GEM / CO correlation slopes for mainland China, South Asia, the Indochinese Peninsula, and Central Asia were $7.3 \pm 4.3$, $7.8 \pm 6.4$, $7.8 \pm 5.0$, and $13.4 \pm 9.5\,\mathrm{pg\,m^{-3}\,ppb^{-1}}$, respectively, and values in the same source regions were $33.3 \pm 30.4$, $27.4 \pm 31.0$, $23.5 \pm 15.3$, and $20.5 \pm 10.0\,\mathrm{pg\,m^{-3}\,ppb^{-1}}$ for the GEM / $CH_4$ correlation slopes, respectively. The geometric means of GEM / $CO_2$ correlation slopes for mainland China, South Asia, and Central Asia were $240 \pm 119$, $278 \pm 164$, $315 \pm 289\,\mathrm{pg\,m^{-3}\,ppm^{-1}}$, respectively. These values were the first reported correlation slopes of GEM / CO, GEM / $CO_2$, and GEM / $CH_4$ in four important source regions of Asia, not including the GEM / CO ratios in mainland China. The correlation slopes of GEM / CO, GEM / $CO_2$, and GEM / $CH_4$ in Asia were relatively higher than those observed in Europe, North America, and South Africa, which may highlight GEM emissions from nonferrous smelting, large-scale and artisanal mercury and gold production, natural sources, and historically deposited mercury (re-emission) in Asia. Using the observed GEM / CO and GEM / $CO_2$ slopes, and the recently reported emission inventories of CO and $CO_2$, the annual GEM emissions in mainland China, South Asia, the Indochinese Peninsula, and Central Asia were estimated to be in the ranges of 1071–1187, 340–470, 125, and 54–90 t, respectively. The estimated quantity of GEM emissions from the GEM / $CH_4$ correlation slopes is significantly larger, which may be due to the larger uncertainties in $CH_4$ emissions in Asia as well as insufficient observations of GEM / $CH_4$ correlation slopes, therefore leading to an overestimate of GEM emissions. Our estimates of GEM emissions in the four Asian regions were significantly higher (3–4 times) than the anthropogenic GEM emissions reported in recent studies. This discrepancy could come from a combination of reasons including underestimates of anthropogenic and natural GEM emissions; large uncertainties related to CO, $CO_2$, and $CH_4$ emission inventories; and inherent limitations of the correlation slope method.

**Published by Copernicus Publications on behalf of the European Geosciences Union.**

## 1 Introduction

Mercury (Hg) is a persistent pollutant in the environment and poses risks for human health risks, mainly through consumption of fish. Due to primary emissions and re-emissions of Hg from anthropogenic sources, the global atmospheric Hg budget has increased significantly since the Industrial Revolution (Mason et al., 1994). There are three major operationally defined Hg forms in the atmosphere, namely gaseous elemental mercury (GEM), gaseous oxidized mercury (GOM), and particulate-bound mercury (PBM). Knowledge on the anthropogenic and natural emissions of Hg into the atmosphere is important for a better understanding of Hg fate in the natural environment (Lindberg et al., 2007). Since the late 1980s, studies have been carried out to investigate the spatial and temporal characteristics of Hg emissions from anthropogenic (Nriagu, 1989; Pirrone et al., 1996; Pacyna et al., 2003; Streets et al., 2005; Pacyna et al., 2010; Pirrone et al., 2010; Streets et al., 2009) and natural sources (Lindberg et al., 1998; Gustin et al., 1999; Gustin et al., 2000; Gustin, 2003; Shetty et al., 2008). Improved emission factors for estimating Hg release from different source categories have significantly reduced the uncertainties (typically < 40 %) of recently reported anthropogenic emissions (Lindberg et al., 2007; Pacyna et al., 2010; Pirrone et al., 2010). The natural emissions (including primary natural emissions and re-emissions of historically deposited Hg), however, still have large uncertainties due to poor understanding of process mechanisms and a lack of reliable data on $Hg^0$ air–surface exchange (Gustin et al., 2005; Schroeder et al., 2005; Selin et al., 2007; Zhang et al., 2009).

Asia is the largest anthropogenic source region of Hg. It contributes approximately two-thirds of global total anthropogenic Hg emissions (Pacyna et al., 2010; Pirrone et al., 2010). Significant progresses have been made in the estimate of anthropogenic Hg emissions in China (Streets et al., 2005; Wu et al., 2006; Tian et al., 2011; Liang et al., 2013). The most recent estimate suggests that total anthropogenic Hg emissions in China increased to 1028 t in 2007 (Liang et al., 2013), nearly 2-fold higher than that in 1995 (Streets et al., 2005). In contrast, anthropogenic Hg emissions in other Asian countries (e.g., South Asia, Southeast Asia, and Central Asia) have received little attention. Such a lack of information limits the development of Hg emission inventories in a globally important source region. Due to the rapid economic development, anthropogenic Hg emissions in these regions are expected to considerably contribute to the regional Hg release (Pacyna et al., 2010).

Estimation of Hg emissions using observed concentrations of atmospheric GEM and other trace gases is a relatively novel approach for studying regional atmospheric Hg budgets. This method was first employed for estimating GEM emissions in the northeastern USA using the GEM / $CO_2$ correlation slopes (Lee et al., 2001). The approach was further improved and then applied for estimating Hg emissions in Asia, Europe, and South Africa (Jaffe et al., 2005; Slemr et al., 2006; Brunke et al., 2012). Such a measurement-based method complements the regional emission inventories estimated by means of conventional statistical approaches. It also yields an estimate of total Hg emissions from both anthropogenic and natural sources (Jaffe et al., 2005; Slemr et al., 2006). In the present study, the correlations slopes of GEM / CO, GEM / $CO_2$, and GEM / $CH_4$ were investigated using the long-term atmospheric measurements at three remote stations in northwestern and southwestern China. The correlation slopes were classified into four source regions in Asia (mainland China, South Asia, the Indochinese Peninsula, and Central Asia) through trajectory analysis for estimating atmospheric Hg emissions. This aim of this work is to fill the knowledge gaps in our understanding on Asian Hg emissions.

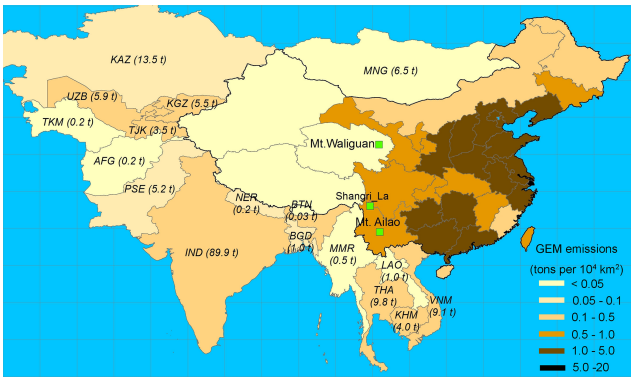


**Figure 1.** Locations of the three ground-based remote sites in northwestern and southwestern China as well as the annual anthropogenic GEM emission for studied Asian countries (Wu et al., 2006; AMAP/UNEP, 2013).

## 2 Experimental

### 2.1 Observational sites

In this study, observations were conducted at three remote sites in northwestern and southwestern China: Mt. Waliguan Baseline Observatory, Shangri-La station, and Mt. Ailao station (Fig. 1). The Mt. Waliguan observatory (WLG; 100.898° E, 36.287° N; 3816 m a.s.l.) is one of the World Meteorological Organization's (WMO) Global Atmospheric Watch (GAW) Baseline Stations, and is situated at the summit of Mt. Waliguan at the edge of northeastern part of the Qinghai–Xizang (Tibet) Plateau. WLG is relatively isolated from industrial point sources and populated regions. The surrounding areas of WLG are naturally preserved arid/semi-arid lands and scattered grasslands and there is no local Hg source around the station. Most of the Chinese industrial and populated regions which may be related to anthropogenic Hg emissions are situated to the east of WLG. Due to the influ-

ence of the Qinghai-Xizang (Tibet) Plateau; the predominate wind directions are from the west to southwest sector in cold seasons and the east sector in warm seasons. As shown in Fig. 1, the three provinces of Qinghai, Xinjiang, and Xizang, have fairly low anthropogenic emissions of Hg, CO, $CO_2$, and $CH_4$ relative to eastern China, Central Asia, and South Asia (Wu et al., 2006; Zhao et al., 2012b; Zhao et al., 2012a; Zhang et al., 2014a; Kurokawa et al., 2013). Therefore, anthropogenic emissions in these three Chinese provinces are expected to have a minimal effect on the westerly and southwesterly airflows in cold seasons, which in turn largely reflects the feature of long-range atmospheric transport of air pollutants from Central Asia and South Asia to WLG.

The Shangri-La station (XGL; 99.733° E, 28.017° N; 3580 m a.s.l.) is located in the Hengduan Mountains area in the southeastern Tibetan Plateau, southwestern China (Fig. 1). The shortest distances from XGL to South Asia and the Indochinese Peninsula are 260 and 100 km, respectively. XGL is surrounded by naturally preserved forest and mountainous areas. There are no large point sources within 100 km of the station with the exception of the city of Shangri-La, which is situated 30 km to the south of the station, with a population of about 140 000, and may be related to anthropogenic emissions of Hg and other air pollutants. Areas to the west and south of the station are well-preserved mountainous forest and have no significant anthropogenic sources. The long-range transport of air masses from South Asia and the Indochinese Peninsula to XGL is not likely impacted by these areas.

The Mt. Ailao station (MAL; 100.017° E, 24.533° N; 2450 m a.s.l.) is located at a summit of the north side of Ailao Mountain National Nature Reserve in central Yunnan province, southwestern China. The reserve stretches more than 130 km from south to north with a maximum width of approximately 20 km. More than 85 % of the reserve is covered by preserved forest. MAL is isolated from industrial sources and populated regions in China. Kunming, one of the largest cities in southwestern China, is located 180 km to the northeast of the station. The site is approximately 200 and 600 km away from the Indochinese Peninsula and South Asia, respectively. Most of the Chinese anthropogenic sources of Hg and other air pollutants are located to the north and east of the station, whereas anthropogenic emissions in southern and western Yunnan province are fairly low (Wu et al., 2006; Zhao et al., 2012b; Zhao et al., 2012a; Zhang et al., 2014a; Kurokawa et al., 2013). The wind system at the station is dominated by the India summer monsoon (ISM) in warm seasons and the westerlies surrounding the Tibetan Plateau in cold seasons. The ISM can carry air pollutants from the Indochinese Peninsula and southern China, while the westerlies carry air pollutants from South Asia.

### 2.2 Measurements of GEM, CO, $CO_2$, and $CH_4$

Continuous measurements of atmospheric GEM at WLG, XGL, and MAL were conducted using an automated Hg vapor analyzer (Tekran 2537A/B). This analyzer has been used extensively for atmospheric total gaseous mercury (TGM) measurements worldwide (Ebinghaus et al., 1999; Munthe et al., 2001; Fu et al., 2012a). It combines the pre-concentration of TGM onto gold traps with thermal desorption and cold vapor atomic fluorescence spectrometry detection of GEM. The analyzer has two gold cartridges working in parallel. While one cartridge collects TGM, the other one performs analysis of the collected TGM. The function of the cartridges is then reversed, allowing continuous sampling of ambient air. The analyzer was set up in a temperature-controlled laboratory (15–25 °C). Ambient air was introduced to the inlet of the analyzer through a 25 ft heated Teflon tube (50 °C). Air particulate matter was removed by using two 45 mm diameter Teflon filters (pore size 0.2 µm), which were installed at the inlets of the sampling Teflon tube and analyzer, respectively. The analyzer was programmed to measure atmospheric TGM at the time resolution of 5 min at XGL and MAL and 10 min at WLG with a volumetric sampling flow rate of $\sim 1.5\,\mathrm{L\,min^{-1}}$. The data quality of the analyzer was controlled by periodic (every 25 h) automatic permeation source injections, and the internal permeation source was calibrated every 3–6 months (Fu et al., 2012a). Atmospheric TGM in general consists of GEM and GOM. In most cases in these studies, GOM constitutes a small portion of TGM (< 1 %; Fu et al., 2012a), and a large fraction of GOM was expected to be captured by the sampling Teflon tube and soda lime trap installed at the inlet of the Tekran 2537A/B analyzer (Fu et al., 2010a; Fu et al., 2012b). Hence, the atmospheric TGM measured herein is referred to as GEM throughout the paper. Concentrations of GEM are expressed in $\mathrm{ng\,m^{-3}}$ Standard Temperature and Pressure (STP) with a standard temperature of 273.16 K and pressure of 1013 hPa.

Atmospheric $CO_2$ at WLG was measured using a LI-COR 6251 non-dispersive infrared (NDIR) analyzer, and $CH_4$ and CO were measured using a G1301 (Picarro, USA) and a G1302 (Picarro, USA) cavity ring-down spectroscopy system (CRDS), respectively. Atmospheric $CO_2$ and $CH_4$ at XGL were measured using the G1301 CRDS, and CO was measured by the G1302 CRDS. Detailed information regarding the schematic of the analytical systems, air collections, calibrations, and data processing has been addressed in previous studies (Zhou et al., 2003; Fang et al., 2013). The analytical precisions for the atmospheric $CO_2$, $CH_4$, and CO measurements were approximately $0.07\,\mathrm{\mu mol\,mol^{-1}}$ (ppm), $1.5\,\mathrm{nmol\,mol^{-1}}$ (ppb), and $2.0\,\mathrm{nmol\,mol^{-1}}$ (ppb), respectively. Atmospheric CO concentrations at MAL were measured using a non-dispersive infrared instrument (Thermo Environmental Instruments model 48C) (Jaffe et al., 2005). Periodical zero air and standard CO gases measurements

were conducted to ensure precise measurements of atmospheric CO concentrations.

All data were averaged hourly for correlation analysis. At WLG, data sets were available from October 2007 to September 2009 for GEM and $CO_2$, from July 2008 to September 2009 for $CH_4$, and from January to September 2009 for CO. Datasets for GEM, $CO_2$, and $CH_4$ were available from July to October 2010 and from September to October 2010 for CO at XGL. Only GEM and CO were available at MAL from September 2011 to March 2013. Due to the exchange of $CO_2$ between the atmosphere and the forest canopy, atmospheric $CO_2$ concentrations at XGL exhibited strong diurnal variations. This had a significant impact on the correlation analysis between GEM and $CO_2$. In light of this, we did not study the correlation of GEM to $CO_2$ at XGL.

### 2.3 Method of correlation analysis

Correlation analysis between atmospheric compounds is a novel tool for studying regional emissions strength of atmospheric pollutants. It has been used for estimating emissions of many atmospheric pollutants with data in good agreement with established emissions inventories (Yokouchi et al., 2006; Worthy et al., 2009; Tohjima et al., 2014). This method was developed and first utilized for estimating Hg emissions in Asia using the correlation of GEM to CO during Asian outflow events (Jaffe et al., 2005). Subsequently, correlation slopes between GEM and other trace gases such as $CH_4$, $CO_2$, and halocarbons were also calculated (Slemr et al., 2006; Brunke et al., 2012). These methods are based on assumptions of no chemical and physical losses of air pollutants, as well as constant emission ratios and constant background of air pollutants during atmospheric transport events (Jaffe et al., 2005). In this study, correlations between atmospheric GEM and CO, $CO_2$, and $CH_4$ were utilized to estimate GEM emissions from mainland China, South Asia, the Indochinese Peninsula, and Central Asia on the basis of continuous measurements of atmospheric GEM, CO, $CO_2$, and $CH_4$ at WLG, XGL, and MAL. The three stations are located in remote areas of northwestern and southwestern China and have constant backgrounds of atmospheric pollutants (Fu et al., 2012a; Zhang et al., 2014b). Also, the transport time (typically less than 5 days) of air masses from the source regions to the stations is much shorter than the atmospheric lifetimes of GEM, CO, $CO_2$, and $CH_4$. The multiple correlation relationships help constrain the estimated GEM emissions.

Correlation analysis was conducted by computing the Pearson correlation (orthogonal least-squares correlation) between GEM concentrations and CO, $CO_2$, and $CH_4$ concentrations independently during pollution events when air masses originated from or passed over a source region consistently. These events had GEM concentrations enhanced by at least 0.5 ng m$^{-3}$ and lasted for 8–24 h. Correlation slopes were selected when linear positive correlation was significant ($p>0.01$) with a correlation coefficient ($r^2$) $>0.5$ (significant correlations with negative slopes were excluded). This criterion was to ensure the method assumptions are valid (Jaffe et al., 2005). Figure 2 shows the time series of atmospheric GEM, CO, $CO_2$, and $CH_4$ concentrations during the transport events from 30 January to 2 March in 2009. The temporal variations of GEM were not consistently correlated with those of the three air pollutants because these events were possible impacted by different sources that led to different relative emission strengths of air pollutants. Therefore, the correlation slopes of GEM / CO, GEM / $CO_2$, and GEM / $CH_4$ were calculated individually in this study. In addition, $CH_4$ / CO, $CH_4$ / $CO_2$, and CO / $CO_2$ correlation slopes were calculated during pollution events with $CH_4$ and CO concentrations elevated by at least 10 and 20 ppb, respectively, on the basis of criterion mentioned for GEM / CO, GEM / $CO_2$, and GEM / $CH_4$ correlation slopes. These correlation slopes are useful for constraining $CH_4$, CO, and $CO_2$ emissions in the study regions.

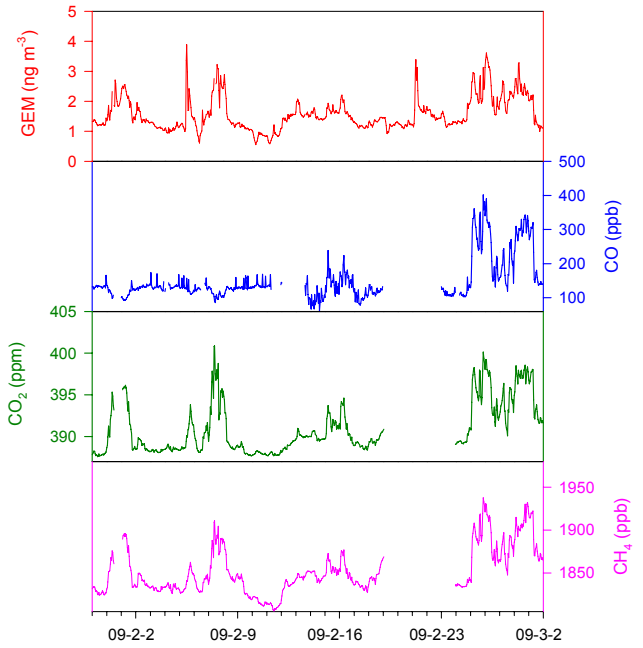


**Figure 2.** A typical example of the consistent variations in GEM, CO, $CO_2$, and $CH_4$ for the period of 30 January to 2 March 2009 at Mt. Waliguan station.

### 2.4 Air mass trajectory calculation

To establish the relationships between the observed correlations slopes and the source regions in Asia, we calculated 5-day backward trajectories every 2 h at each of the stations using the TrajStat Geographical Information System software and gridded meteorological data (Global Data Assimilation System, GDAS1) from the US National Oceanic and Atmospheric Administration (NOAA). The global gridded meteorological data have a horizontal resolution of 1° (360 × 180

grid cells) with 23 vertical levels from 1000 to 20 hPa (Wang et al., 2009). These trajectories ended at a height of 500 m above ground at WLG, XGL, and MAL. The trajectory endpoints in each event were averaged to yield the transport pathway. The source area identified by the trajectory analysis was weighted by the correlation slope observed for the stations during the event.

It should be noted that the endpoints of the backward trajectories can occasionally pass over multiple regions. In this case, we attributed the correlation slopes to the most important source regions that the air masses traveled through. For example, most air masses that originated from and/or passed over South Asia and Central Asia and ended at WLG also passed over the Chinese provinces of Xinjiang, Xizang, and Qinghai, which have fairly low emissions of atmospheric GEM, CO, $CO_2$, and $CH_4$ (Wu et al., 2006; Kurokawa et al., 2013). It is therefore assumed that these air masses carried the emission signals from Central and South Asia. On the other hand, eastern and central China is an important source region of atmospheric GEM, CO, $CO_2$, and $CH_4$, and therefore the air masses passing over eastern and central China were assumed to carry the emission signals in China. For XGL and MAL, the areas to the west and south of the stations in Yunnan province, southwestern China have fairly low emissions of atmospheric GEM, CO, $CO_2$, and $CH_4$ (Wu et al., 2006; Kurokawa et al., 2013). The air masses that passed over South Asia and the Indochinese Peninsula were assumed to carry the emission signals from the respective region.

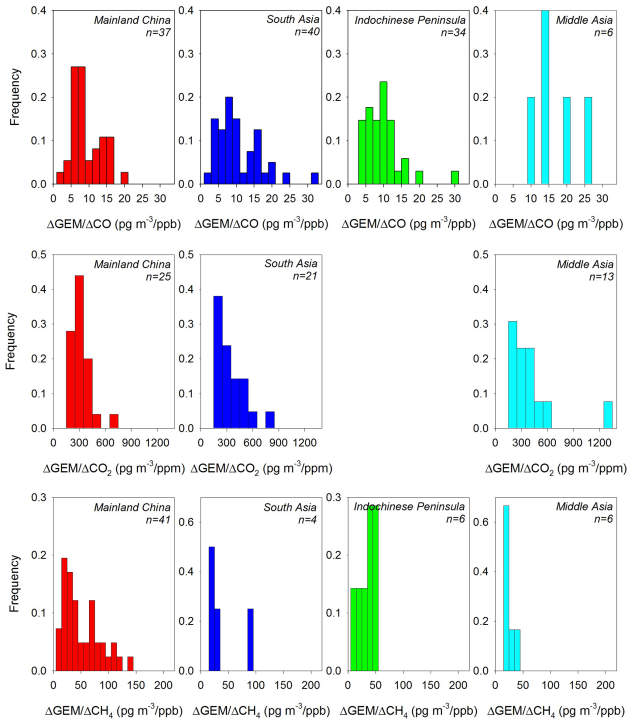


**Figure 3.** Histograms of the correlations slopes of GEM / CO, GEM / $CO_2$, and GEM / $CH_4$ for the four Asian regions during the whole study period. All the correlation slopes meet the selection criteria (see text).

## 3 Results and discussion

### 3.1 Atmospheric GEM concentrations at WLG, XGL, and MAL and potential source regions

Averaged atmospheric GEM concentrations during the study period were $2.05 \pm 0.96\,\mathrm{ng\,m^{-3}}$ (hourly means ranging from 0.40 to $14.58\,\mathrm{ng\,m^{-3}}$, October 2007 to September 2009) for WLG, $2.52 \pm 0.70\,\mathrm{ng\,m^{-3}}$ (hourly means ranging from 1.35 to $5.98\,\mathrm{ng\,m^{-3}}$, from July to October 2010) for XGL, and $2.05 \pm 0.67\,\mathrm{ng\,m^{-3}}$ (hourly means ranging from 0.89 to $6.26\,\mathrm{ng\,m^{-3}}$, from September 2011 to March 2013) for MAL. The levels of atmospheric GEM at the three stations were relatively lower compared to those observed in North America and Europe (1.3–2.0 $\mathrm{ng\,m^{-3}}$; Sprovieri et al., 2010; Lan et al., 2012; Cole et al., 2013; Munthe et al., 2003). A previous study by Fu et al. (2012a) at WLG suggested that long-range atmospheric transport of GEM from industrial and urbanized areas in northwestern China and northwestern India contributed significantly to the elevated GEM at WLG. For GEM at XGL, potential sources areas included northern India, Myanmar, western Sichuan province, and western Yunnan province (Zhang et al., 2014b). The potential source areas varied with monsoon at MAL. During the ISM seasons (May to October), MAL was mainly impacted by emission of Hg from eastern Yunnan, western Guizhou, and southern Sichuan of China and the northern part of the Indochinese Peninsula. During non-ISM seasons, the impact of emissions from India and the northwestern part of the Indochinese Peninsula increased and played an important role in elevated GEM observed at MAL (Zhang et al., manuscript under preparation, 2015).

### 3.2 Observed correlation slopes for the studied source regions

Using backward trajectory analysis, we divided GEM / CO slopes into four regions, GEM / $CO_2$ into three regions, and GEM / $CH_4$ into four regions (Table 1). Histograms of GEM / CO, GEM / $CO_2$, and GEM / $CH_4$ slopes for the identified source regions are displayed in Fig. 3. Most of the correlation slopes followed a lognormal distribution (Table 1). Hence, geometric means of the correlation slopes are used throughout the paper.

The geometric mean correlation slopes of GEM / CO for mainland China, South Asia, the Indochinese Peninsula, and Central Asia were $7.3 \pm 4.3$ (1 SD, $n = 37$), $7.8 \pm 6.4$ (1 SD, $n = 40$), $7.8 \pm 5.0$ (1 SD, $n = 34$), and $13.4 \pm 9.5\,\mathrm{pg\,m^{-3}\,ppb^{-1}}$ (1 SD, $n = 6$), respectively. The observed correlation slopes for mainland China were associated

**Table 1.** Statistical summary of GEM / CO, GEM / $CO_2$, GEM / $CH_4$, $CH_4$ / CO, $CH_4$ / $CO_2$, and CO / $CO_2$ correlation slopes observed for mainland China, South Asia, the Indochinese Peninsula, and Central Asia during the study period.

| Correlation slopes | Identified regions | Slope | | | | | | |
|---|---|---|---|---|---|---|---|---|
| | | Range | Mean | Geo. mean | Median | 1 SD | N | Lognormal K–S test ($p$) |
| GEM / CO | mainland China | 1.4–19.6 | 7.3 | 8.4 | 7.5 | 4.3 | 37 | 0.96 |
| ($pg\,m^{-3}\,ppb^{-1}$) | South Asia | 1.5–31.6 | 7.8 | 9.6 | 7.8 | 6.4 | 40 | 0.92 |
| ($8.0 \times 10^{-4}\,g\,g^{-1}$) | Indochinese Peninsula | 2.8–28.0 | 7.8 | 8.9 | 8.4 | 5.0 | 34 | 0.94 |
| | Central Asia | 2.0–34.0 | 13.4 | 17.0 | 17.0 | 9.5 | 6 | 0.93 |
| GEM / $CO_2$ | mainland China | 115–687 | 248 | 268 | 254 | 119 | 25 | 1.0 |
| ($pg\,m^{-3}\,ppm^{-1}$) | South Asia | 130–743 | 270 | 305 | 266 | 164 | 21 | 0.88 |
| ($5.1 \times 10^{-7}\,g\,g^{-1}$) | Central Asia | 167–1260 | 315 | 374 | 275 | 289 | 13 | 0.97 |
| GEM / $CH_4$ | mainland China | 8.3–110 | 33.3 | 43.4 | 34.9 | 30.4 | 41 | 0.87 |
| ($pg\,m^{-3}\,ppb^{-1}$) | South Asia | 14.5–80.9 | 27.4 | 35.0 | 22.3 | 31.0 | 4 | 0.90 |
| ($1.4 \times 10^{-3}\,g\,g^{-1}$) | Indochinese Peninsula | 7.8–47.7 | 23.5 | 27.7 | 28.8 | 15.3 | 6 | 0.87 |
| | Central Asia | 10.9–39.0 | 20.5 | 22.2 | 18.7 | 10.0 | 6 | 0.85 |
| $CH_4$ / CO | mainland China | 0.05–0.93 | 0.27 | 0.31 | 0.28 | 0.18 | 81 | 0.88 |
| ($ppb\,ppb^{-1}$) | South Asia | 0.21–0.52 | 0.31 | 0.32 | 0.29 | 0.09 | 9 | 0.96 |
| ($0.57\,g\,g^{-1}$) | Indochinese Peninsula | 0.10–0.77 | 0.30 | 0.36 | 0.33 | 0.20 | 13 | 0.76 |
| | Central Asia | 0.13–0.45 | 0.20 | 0.24 | 0.22 | 0.11 | 9 | 0.95 |
| $CH_4$ / $CO_2$ | mainland China | 2.96–24.5 | 6.8 | 7.5 | 6.4 | 4.0 | 36 | 0.86 |
| ($ppb\,ppm^{-1}$) | South Asia | 5.05–12.3 | 7.3 | 7.6 | 6.8 | 2.7 | 12 | 0.28 |
| ($0.36 \times 10^{-3}\,g\,g^{-1}$) | Central Asia | 5.22–23.2 | 8.7 | 9.9 | 8.6 | 5.9 | 9 | 0.69 |
| CO / $CO_2$ | mainland China | 10.1–152 | 29.0 | 32.0 | 27.4 | 20.8 | 43 | 0.29 |
| ($ppb\,ppm^{-1}$) | South Asia | 13.7–75.9 | 22.5 | 26.8 | 20.7 | 20.7 | 8 | 0.68 |
| ($0.64 \times 10^{-3}\,g\,g^{-1}$) | Central Asia | 5.7–30.9 | 16.8 | 16.4 | 14.5 | 8.4 | 8 | 0.89 |

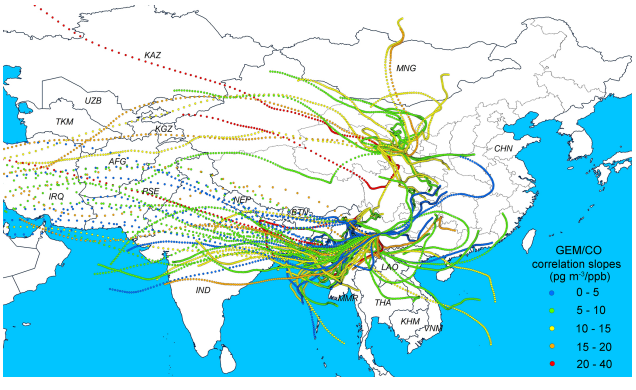


**Figure 4.** Correlation slopes of GEM / CO at the three monitoring sites and associated origins of airflows.

with air masses originating from northwestern, southwestern, central, and southern China (Fig. 4). The trajectories were simulated for a period of 5 days and were therefore expected to pass over most of mainland China because of the length of the trajectories. As a result, these observed correlation slopes of GEM / CO for northwestern, southwestern, central, and southern China were likely representative of the emissions from a majority of areal coverage of mainland China. The correlation slopes of GEM / CO observed for South Asia, the Indochinese Peninsula, and Central Asia are also representative of these regions as the air masses pass over a majority of these regions (Fig. 4).

GEM / CO correlation slopes were comparable among mainland China, South Asia, and the Indochinese Peninsula (means range from 7.3 to 7.8 $pg\,m^{-3}\,ppb^{-1}$), but nearly 2-fold lower than the mean for Central Asia (mean $= 13.4 \pm 9.5\,pg\,m^{-3}\,ppb^{-1}$). This trend is consistent with the anthropogenic emission ratios of GEM to CO in different regions of Asia. Based on the published anthropogenic GEM and CO emissions inventories in Asia (Kurokawa et al., 2013; AMAP/UNEP, 2013; Wu et al., 2006), we calculated the anthropogenic GEM / CO emission ratio to be 7.2 $pg\,m^{-3}\,ppb^{-1}$ ($5.8 \times 10^{-6}\,g\,g^{-1}$) for Central Asia, which is significantly higher than those ratios for mainland China (2.7 $pg\,m^{-3}\,ppb^{-1}$; $2.2 \times 10^{-6}\,g\,g^{-1}$), South Asia (1.6 $pg\,m^{-3}\,ppb^{-1}$; $1.3 \times 10^{-6}\,g\,g^{-1}$), and the Indochinese Peninsula (1.5 $pg\,m^{-3}\,ppb^{-1}$; $1.2 \times 10^{-6}\,g\,g^{-1}$) (Table 2). Although correlation slopes of GEM / CO were also likely influenced by secondary emissions of GEM (Jaffe et al., 2005; Slemr et al., 2006), the higher anthro-

**Table 2.** Anthropogenic emissions GEM, CO, $CO_2$, and $CH_4$ in mainland China, South Asia, the Indochinese Peninsula, and Central Asia, as well as estimated anthropogenic emission ratios.

| Regions | Anthropogenic emissions | | | | Estimated emission ratios | | | | |
|---|---|---|---|---|---|---|---|---|---|
| | GEM ($t\,yr^{-1}$) | CO ($\times 10^6\,t\,yr^{-1}$) | $CO_2$ ($\times 10^6\,t\,yr^{-1}$) | $CH_4$ ($\times 10^6\,t\,yr^{-1}$) | GEM / CO ($pg\,m^{-3}\,ppb^{-1}$) | GEM / $CO_2$ ($pg\,m^{-3}\,ppm^{-1}$) | GEM / $CH_4$ ($pg\,m^{-3}\,ppb^{-1}$) | $CH_4$ / CO ($ppb\,ppb^{-1}$) | $CH_4$ / $CO_2$ ($ppb\,ppm^{-1}$) | CO / $CO_2$ ($ppb\,ppm^{-1}$) |
| Mainland China | 394.9[a] | 183.0[b] | 9370[c] | 39.6[d] | 2.7 | 82.4 | 7.1 | 0.38 | 11.6 | 30.7 |
| South Asia | 96.3[a] | 75.2[e] | 2460[e] | 39.3[e] | 1.6 | 76.5 | 1.8 | 0.91 | 43.8 | 48.1 |
| Indochinese Peninsula | 24.4[a] | 19.9[e] | 557[e] | 14.9[e] | 1.5 | 85.7 | 1.2 | 1.31 | 73.5 | 56.2 |
| Central Asia | 28.8[a] | 5.0[e] | 562[e] | 7.5[e] | 7.2 | 102 | 2.8 | 2.62 | 36.7 | 14.0 |

[a] (AMAP/UNEP, 2013), [b] (Zhao et al., 2012b), [c] (Zhao et al., 2012a), [d] (Zhang and Chen, 2010), [e] (Kurokawa et al., 2013).

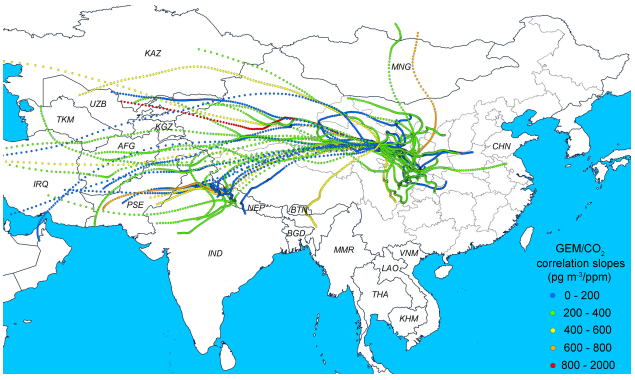


**Figure 5.** Correlation slopes of GEM / $CO_2$ at WLG and associated origins of airflows.

pogenic GEM / CO emission ratio in Central Asia partially explains the elevated correlation slopes of GEM / CO in the region. The GEM / CO correlation slopes for mainland China were slightly higher than those for Chinese outflows observed at Hedo Station, Okinawa, Japan; Mt. Bachelor Observatory (MBO), western USA; and Seoul, Korea (4.6–7.4 $pg\,m^{-3}\,ppb^{-1}$), as well as from coastal flight observations (Jaffe et al., 2005; Weiss-Penzias et al., 2007; Choi et al., 2009; Pan et al., 2006; Friedli et al., 2004), but slightly lower than values observed in the air masses that originated from and/or passed over eastern China (8.0 and 11.4 $pg\,m^{-3}\,ppb^{-1}$) (Friedli et al., 2004; Sheu et al., 2010) and those in the upper troposphere observed during the flights from Frankfurt, Germany, to Guangzhou, southern China (8.2–12.8 $pg\,m^{-3}\,ppb^{-1}$) (Slemr et al., 2009; Slemr et al., 2014). The difference between the present study and literature values may reflect a regional emission difference. The correlation slopes calculated from the observations in mainland China were associated with air masses originated from and passed over northwestern, southwestern, central, and southern China (Fig. 4), whereas those estimated in previous studies were associated with the air masses in eastern China. Furthermore, there may be impacts from recent changes in atmospheric sources of GEM, including the decreasing contributions of GEM emissions from domestic coal, agricultural residual, and forest burning emissions to the total anthropogenic emissions in mainland China during the past decade (Wu et al., 2006; Liang et al., 2013). These sources were reported with relatively lower GEM / CO emission ratios compared to other industrial sources (Weiss-Penzias et al., 2007; Zhang et al., 2013). Apart from the study of Sheu et al. (2010), in which a GEM / CO correlation slope (5.0 $pg\,m^{-3}\,ppb^{-1}$) for the outflow from the Indochinese Peninsula was reported, there have been few studies regarding the correlation slopes of GEM / CO in South Asia, the Indochinese Peninsula, and Central Asia.

The geometric means of GEM / $CO_2$ correlation slopes for mainland China, South Asia, and Central Asia were

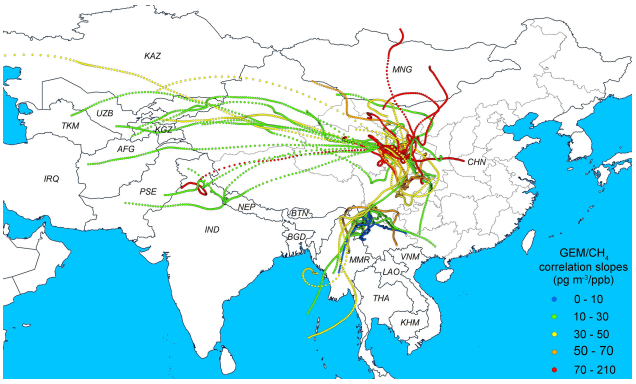


**Figure 6.** Correlation slopes of GEM / $CH_4$ at WLG and XGL and associated origins of airflows.

$248 \pm 119$ (1 SD, $n = 25$), $270 \pm 164$ (1 SD, $n = 21$), and $315 \pm 289$ pg m$^{-3}$ ppm$^{-1}$ (1 SD, $n = 13$), respectively. The GEM / $CO_2$ correlation slopes calculated from the observations in mainland China were associated with air masses originating from northwestern and southwestern China, as well as from central China (Fig. 5). The GEM / $CO_2$ correlation slopes associated with trajectories transported from South Asia predominantly came from Pakistan and northwestern India, covering a large area of Central Asia (Fig. 5). The values of GEM / $CO_2$ correlation slopes also vary with regions, with the greatest geometric mean GEM / $CO_2$ for the Central Asia. The spatial pattern of GEM / $CO_2$ slopes appeared to be consistent with the anthropogenic emission ratios of GEM to $CO_2$ in Asia. With the anthropogenic emissions of GEM and $CO_2$ taken into account (Wu et al., 2006; Kurokawa et al., 2013; AMAP/UNEP, 2013), GEM / $CO_2$ emission ratios of anthropogenic sources were on the order of $5.1 \times 10^{-8}$ t t$^{-1}$ in Central Asia and $4.2 \times 10^{-8}$ t t$^{-1}$ in mainland China, and $3.9 \times 10^{-8}$ t t$^{-1}$ in South Asia.

The geometric means of the correlation slopes of GEM / $CH_4$ for mainland China, South Asia, the Indochinese Peninsula, and Central Asia were $33.3 \pm 30.4$ (1 SD, $n = 41$), $27.4 \pm 31.0$ (1 SD, $n = 4$), $23.5 \pm 15.3$ (1 SD, $n = 6$), and $20.5 \pm 10.0$ pg m$^{-3}$ ppb$^{-1}$ (1 SD, $n = 6$), respectively. Forty-one GEM / $CH_4$ ratios were calculated in mainland China (26 at the WLG site and 15 at the XGL site). The correlation slopes of GEM / $CH_4$ at WLG were associated with the air masses from northwestern China and those at XGL were associated with the air masses from Yunnan province, southwestern China (Fig. 6). The events of air transport from South Asia, the Indochinese Peninsula, and Central Asia (4–6 slopes for each region) were relatively fewer. The air masses related to the slopes for South Asia and the Indochinese Peninsula were from northwestern India and Myanmar, respectively. The GEM / $CH_4$ ratios calculated from the observations in the air masses from different regions in mainland China varied significantly (Fig. 6). The GEM / $CH_4$ ratios associated with the air masses from northwestern China fell within the range of 14.6–208 pg m$^{-3}$ ppb$^{-1}$ (geometric mean = 49 pg m$^{-3}$ ppb$^{-1}$), significantly higher than those from southwestern China (ranging from 8 to 69 pg m$^{-3}$ ppb$^{-1}$, geometric mean = 20 pg m$^{-3}$ ppb$^{-1}$). The lower GEM / $CH_4$ values estimated from the air transport from southwestern China are likely due to the $CH_4$ emissions from rice paddies and natural wetlands (Zhang and Chen, 2010; Chen et al., 2013; Zhang et al., 2014a). The anthropogenic release of GEM into the atmosphere in the region is relatively lower (Fu et al., 2012c).

The geometric means of the correlation slopes of $CH_4$ / CO for mainland China, South Asia, the Indochinese Peninsula, and Central Asia were $0.27 \pm 0.18$ (1 SD, $n = 81$), $0.31 \pm 0.09$ (1 SD, $n = 9$), $0.30 \pm 0.20$ (1 SD, $n = 13$), and $0.20 \pm 0.11$ ppb ppb$^{-1}$ (1 SD, $n = 9$), respectively. The geometric means of the correlation slopes of $CH_4$ / $CO_2$ for mainland China, South Asia, and Central Asia were $6.8 \pm 4.0$ (1 SD, $n = 36$), $7.3 \pm 2.7$ (1 SD, $n = 12$), and $8.7 \pm 5.9$ ppb ppm$^{-1}$ (1 SD, $n = 9$), respectively. The geometric means of the CO / $CO_2$ correlation slopes for mainland China, South Asia, and Central Asia were $29.0 \pm 20.8$ (1 SD, $n = 43$), $22.5 \pm 20.7$ (1 SD, $n = 8$), and $16.8 \pm 8.4$ ppb ppm$^{-1}$ (1 SD, $n = 8$) , respectively. The observed correlation slopes for $CH_4$ / CO, $CH_4$ / $CO_2$, and CO / $CO_2$ in the studied regions were higher than that obtained for South Africa (Brunke et al., 2012). Note that observed $CH_4$ / CO and $CH_4$ / $CO_2$ correlation slopes were lower than anthropogenic emission ratios of $CH_4$ / CO and $CH_4$ / $CO_2$, while observed CO / $CO_2$ correlation slopes were consistent with anthropogenic emission ratios of CO to $CO_2$ (with the exception of South Asia, Table 1 and Table 2). This indicates that the anthropogenic inventories may overestimate the $CH_4$ emissions in the studied regions.

### 3.3 Implications of atmospheric Hg emission sources in Asia

The correlation slopes of GEM / CO, GEM / $CO_2$, and GEM / $CH_4$ were similar in Asian regions. This indicates that the sources of atmospheric Hg were more or less similar among the four studied regions. The GEM / CO, GEM / $CO_2$, and GEM / $CH_4$ correlation slopes in Asian were higher than those observed in other regions. For example, the GEM / CO ratios in Europe, South Africa, and North America were in the range of 0.3–5.0 pg m$^{-3}$ ppb$^{-1}$ (Jaffe et al., 2005; Slemr et al., 2006; Brunke et al., 2012). For GEM / $CO_2$ ratios, previous studies reported a mean of 184 pg m$^{-3}$ ppm$^{-1}$ for the northeastern USA and 63 pg m$^{-3}$ ppm$^{-1}$ for South Africa (Lee et al., 2001; Brunke et al., 2012). The mean GEM / $CH_4$ ratios in Europe and South Africa were 3.9 and 3.6 pg m$^{-3}$ ppb$^{-1}$, respectively (Slemr et al., 2006; Brunke et al., 2012), approximately 1 order of magnitude lower than those in Asia.

Non-ferrous metal smelting (zinc, lead, and gold production), coal combustion, cement production, and mercury

production are the four largest source categories of anthropogenic GEM emissions in mainland China. Emission factors (EFs) of CO and $CO_2$ from anthropogenic sources have been investigated extensively. In this study, the EFs of CO and $CO_2$ summarized from Zhao et al. (2012a) and Zhao et al. (2012b) were adopted for calculating GEM / CO and GEM / $CO_2$ emission ratios for anthropogenic sources. EFs of GEM from coal combustion, non-ferrous smelting, cement, primary mercury production, and large-scale gold production have also be reported (Streets et al., 2005; Wang et al., 2010; Li et al., 2010; Pacyna et al., 2010). The emission ratios of GEM / $CH_4$ were not estimated due to the fact that GEM and $CH_4$ do not have common emission sources. The estimated emission ratio of GEM / CO is 149 pg $m^{-3}$ $ppb^{-1}$ for zinc smelting, 120 pg $m^{-3}$ $ppb^{-1}$ for lead smelting, 0.6 pg $m^{-3}$ $ppb^{-1}$ for coal combustion, 0.3 pg $m^{-3}$ $ppb^{-1}$ for cement production, $6.7 \times 10^3$ pg $m^{-3}$ $ppb^{-1}$ for primary mercury production, and $870 \times 10^3$ pg $m^{-3}$ $ppb^{-1}$ for large-scale gold production. The estimated emission ratio of GEM / $CO_2$ is $48 \times 10^3$ pg $m^{-3}$ $ppm^{-1}$ for zinc smelting, $131 \times 10^3$ pg $m^{-3}$ $ppm^{-1}$ for lead smelting, 10 pg $m^{-3}$ $ppm^{-1}$ for coal combustion, and 36 pg $m^{-3}$ $ppm^{-1}$ for cement production, $190 \times 10^3$ pg $m^{-3}$ $ppm^{-1}$ for primary mercury production, and $240 \times 10^5$ pg $m^{-3}$ $ppm^{-1}$ for large-scale gold production. It should be pointed out that artisanal and small-scale gold and mercury production is also important sources of atmospheric GEM in Asia (Pacyna et al., 2010; Muntean et al., 2014). These two sources are generally equipped with poor Hg-control devices and are expected to produce much larger emission ratios of GEM / CO and GEM / $CO_2$ (Li et al., 2009; Muntean et al., 2014). Biomass burning (forest and grassland fires, crop residual burning, and crop residues and wood combustion) is also an important atmospheric GEM source in mainland China (Huang et al., 2011). The observed GEM / CO and GEM / $CO_2$ emission ratios for biomass burning were 0.6–2.1 and 109 pg $m^{-3}$ $ppm^{-1}$, respectively (Brunke et al., 2001; Friedli et al., 2003; Weiss-Penzias et al., 2007; Ebinghaus et al., 2007). Given that non-ferrous smelting and mercury production are important sources of atmospheric GEM in Asia and have relatively higher GEM / CO and GEM / $CO_2$ emission ratios, the elevated GEM / CO and GEM / $CO_2$ correlation slopes in Asia are likely to have resulted from these emission sources. None of the GEM / CO and GEM / $CO_2$ emission ratios from anthropogenic sources agree consistently with the observed correlation slopes, indicating that the observed correlation slopes of GEM / CO and GEM / $CO_2$ were likely influenced by multiple sources, including release from natural surfaces.

Anthropogenic emission alone is not able to fully explain the observed correlation slopes. Based on the annual anthropogenic emission inventories of GEM, CO, $CO_2$, and $CH_4$, the emission ratios of GEM / CO, GEM / $CO_2$, and GEM / $CH_4$ were calculated; results are shown in Table 2. The anthropogenic emission ratios were all significantly lower than the correlation slopes of observed concentrations. The discrepancy was partially attributed to the fact that observed correlation slopes were not uniformly distributed within different regions and seasons, which may be not adequate to represent the annual and overall characteristics of the emission ratios in the studied regions. Unfortunately, this reason cannot be evaluated further due to the lack of seasonal assessments of the GEM, CO, $CO_2$, and $CH_4$ emissions. In addition, it is speculated that contributions from soil emission of GEM may play a crucial role. Soil emissions are an important source of atmospheric GEM (Pirrone et al., 2010). Due to the lack of soil GEM flux measurements from South Asia, the Indochinese Peninsula, and Central Asia, the measurements in China were applied for the analysis. The measured soil GEM fluxes in southwestern and southern China fell within the ranges of 19.2–132 (mean = 49 ng $m^{-2}$ $h^{-1}$) and 18.2–114 ng $m^{-2}$ $h^{-1}$ (mean = 43 ng $m^{-2}$ $h^{-1}$), respectively (Feng et al., 2005; Fu et al., 2008, 2012c). These values are significantly higher than those in Europe and North America (Zhang et al., 2001; Ericksen et al., 2006; Schroeder et al., 2005). Assuming the soil emissions of $CO_2$ in mainland China are comparable to those in Europe and North America, the elevated GEM emission fluxes from soil in China can lead to the GEM / CO and GEM / $CO_2$ correlation slopes in mainland China. Using the published $CO_2$ emission fluxes from subtropical arable soil (Lou et al., 2004), we calculated the soil GEM / $CO_2$ emission ratios to be 148–1070 pg $m^{-3}$ $ppm^{-1}$ (mean = 370 pg $m^{-3}$ $ppm^{-1}$). Given that soil does not release significant CO into the atmosphere (EC-JRC/PBL, 2011), soil emissions are expected to produce extremely high GEM / CO emission ratios. Rice paddies are sources of both GEM and $CH_4$. However, previous studies suggested that GEM emission fluxes from rice paddies were much lower compared to those of bare soils, in the range of 1.4–23.8 ng $m^{-2}$ $h^{-1}$ (Zhu et al., 2011; Fu et al., 2012c). The mean $CH_4$ emission flux in China has been recorded as high as 11.4 mg $m^{-2}$ $h^{-1}$ (Chen et al., 2013). This yields average GEM / $CH_4$ emission ratios of 0.1–1.5 pg $m^{-3}$ $ppb^{-1}$ from rice paddies. The low GEM / $CH_4$ emission ratios from rice paddies were opposite to our observations, indicating that they is not the cause of elevated GEM / $CH_4$ slopes in China. However, bare soils are not expected to release $CH_4$ and should produce extremely high GEM / $CH_4$ emission ratios. Given the larger areas and higher GEM fluxes of bare soils in China, elevated GEM / $CH_4$ correlation slopes in China are probably caused by dry soil GEM emissions.

### 3.4 Estimates of GEM emissions

GEM emissions in mainland China, South Asia, the Indochinese Peninsula, and Central Asia were calculated using the GEM / CO, GEM / $CO_2$, and GEM / $CH_4$ correlation slopes obtained in the present study as well as emissions of CO, $CO_2$, and $CH_4$ in Asian countries. Emissions of CO, $CO_2$,

**Table 3.** Estimates of GEM emissions from mainland China, South Asia, the Indochinese Peninsula, and Central Asia using the observed correlation slopes and CO, $CO_2$, and $CH_4$ inventories. A comparison to anthropogenic inventories is also included.

| Asian regions | CO emission ($\times 10^6$ t yr$^{-1}$) | $CO_2$ emission ($\times 10^6$ t yr$^{-1}$) | $CH_4$ emission ($\times 10^6$ t yr$^{-1}$) | Estimated GEM emission (t yr$^{-1}$) from GEM / CO slopes | from GEM / $CO_2$ slopes | from GEM / $CH_4$ slopes | Anthropogenic GEM emission (t yr$^{-1}$) |
|---|---|---|---|---|---|---|---|
| Mainland China | 183[a] | 9370[b] | 39.6[c] | 1071 | 1187 | 1846 | 375–430[e] |
| South Asia | 75.2[d] | 2461[d] | 39.3[d] | 470 | 340 | 575 | 96[f] |
| Indochinese Peninsula | 20.0[d] | 557[d] | 15.0[d] | 125 | – | 493 | 24[f] |
| Central Asia | 5.0[d] | 562[d] | 7.5[d] | 54 | 90 | 215 | 29[f] |

[a] Zhao et al. (2012b), [b] Zhao et al. (2012a), [c] Zhang and Chen (2010), [d] Kurokawa et al. (2013), [e] Wu et al. (2006), [f] AMAP/UNEP (2013).

and $CH_4$ in South Asia, the Indochinese Peninsula, and Central Asia were adopted from the study by Kurokawa et al. (2013), which in most cases are consistent with those reported by EDGAR 4.2 (EC-JRC/PBL, 2011). Emissions of CO, $CO_2$, and $CH_4$ in mainland China were adopted from Chinese studies (Table 3). The emissions of CO and $CO_2$ in these studies agree with others reported in the literature (EC-JRC/PBL, 2011; Kurokawa et al., 2013; Liu et al., 2013; Tohjima et al., 2014). The $CH_4$ emission used for mainland China in this study ($39.6 \times 10^6$ t yr$^{-1}$) is significantly lower than those emissions reported by Kurokawa et al. (2013) and EDGAR 4.2 (EC-JRC/PBL, 2011) (73.2–76.0 $\times 10^6$ t yr$^{-1}$) but similar to that predicted from $CH_4$ / $CO_2$ correlations at Hateruma Island ($46.0 \times 10^6$ t yr$^{-1}$) (Tohjima et al., 2014). The Chinese studies utilized optimized emission factors for many sources (e.g., coal mining, rice cultivation, enteric fermentation) and are expected to give a better prediction of $CH_4$ emissions in China (Cheng et al., 2011; Chen et al., 2013).

Annual GEM emissions estimated from GEM / CO correlation slopes were 1071, 470, 125, and 54 t yr$^{-1}$ for mainland China, South Asia, the Indochinese Peninsula, and Central Asia, respectively. The estimated GEM emissions from GEM / $CO_2$ correlation slopes are similar to those derived from GEM / CO correlation slopes, with annual GEM emissions of 1187, 340, and 90 t yr$^{-1}$ for mainland China, South Asia, and Central Asia (no correlation slopes were observed for the Indochinese Peninsula). GEM emissions estimated from GEM / $CH_4$ correlation slopes were substantially higher than those derived from GEM / CO and GEM / $CO_2$ correlation slopes (Table 3). For example, the estimated GEM emission in China based on GEM / $CH_4$ ratios reached 1846 t yr$^{-1}$, 55–72 % higher than those estimated from GEM / CO and GEM / $CO_2$ ratios. Similarly, the estimated GEM emissions in South Asia, the Indochinese Peninsula, and Central Asia from GEM / $CH_4$ ratios were 1.2–3.9 times greater than those estimated from GEM / CO and GEM / $CO_2$ ratios.

The discrepancy in GEM emissions might be due to the following reasons. First, it was reported that $CH_4$ emissions in China and other Asian counties have larger uncertainties compared to CO and $CO_2$ emissions (Olivier et al., 2001; Kurokawa et al., 2013). Recent Chinese studies have suggested that the $CH_4$ emissions in China reported by previous studies were overestimated by a factor of $\sim 2$ (Zhang and Chen, 2010; Cheng et al., 2011; Chen et al., 2013; Kurokawa et al., 2013). This may also be the case for South Asia, the Indochinese Peninsula, and Central Asia. As shown in Tables 1 and 2, the observed $CH_4$ / CO and $CH_4$ / $CO_2$ correlation slopes for the studied regions were significantly higher than the emission ratios calculated on basis of published inventories, while CO / $CO_2$ correlation slopes were consistent with the emission ratios. This implies that previously reported $CH_4$ emissions in the studied regions were likely overestimated, which may partially explain the overestimated GEM emissions derived from GEM / $CH_4$ correlation slopes and $CH_4$ emissions. Secondly, we do not obtain substantial correlation slopes of GEM / $CH_4$, which might be not representative for the studied regions. Using mainland China as the example, 26 out of 41 slopes were observed at WLG. The slopes were related to air masses that originated from and/or passed over northwestern China, which yielded a mean GEM / $CH_4$ correlation slope of $49 \pm 30.0$ pg m$^{-3}$ ppb$^{-1}$, significantly higher than that of the slopes from southwestern China ($20.0 \pm 19.1$ pg m$^{-3}$ ppb$^{-1}$). The slopes associated with air masses from northwestern China were expected to be predominantly influenced by emissions of GEM and $CH_4$ its proximity to WLG. Previous studies have suggested that the anthropogenic emission ratios of GEM / $CH_4$ in northwestern China were relatively higher than the values from other Chinese regions (Wu et al., 2006; Zhang et al., 2014a). Therefore, the large fraction of slopes obtained from northwestern China was also responsible for overestimates of GEM emissions in the present study. Hence, it is speculated that GEM / CO and GEM / $CO_2$ correlation slopes may better depict the GEM emissions in Asia than GEM / $CH_4$ correlation slopes in the present study.

The estimated GEM emissions in mainland China, South Asia, the Indochinese Peninsula, and Central Asia using GEM / CO and GEM / $CO_2$ ratios agree reasonably with

the results of previous studies (Jaffe et al., 2005; Weiss-Penzias et al., 2007), but are consistently greater than the reported anthropogenic GEM emissions (Table 3). The estimated GEM emissions in China are about 3–4-fold higher than the anthropogenic emission for 2003–2010 (Wu et al., 2006; AMAP/UNEP, 2013; Muntean et al., 2014), and those in South Asia, the Indochinese Peninsula, and Central Asia are 2–5-fold higher than the anthropogenic emissions for 2010 (AMAP/UNEP, 2013). It is hypothesized that underestimates of anthropogenic GEM emissions, contributions of re-emission and natural emissions, uncertainties in the fraction of Hg species in the inventory, and conversion of Hg species during long-range transport are reasons for the discrepancy (Jaffe et al., 2005; Slemr et al., 2006). A recent study showed that the total anthropogenic Hg emissions in China increased to 1028 t in 2007, which is about 50 % higher than that in 2003 and corresponds to a mean annual rate of increase of 10.6 % (Wu et al., 2006; Liang et al., 2013). If this rate of increase is applied to the estimate of anthropogenic GEM emissions in 2003 (Wu et al., 2006), anthropogenic GEM emission in China is expected to be 800 t for 2010. This value is significantly higher than the estimate in 2003 as well as the value from the UNEP report for 2010 (430 t) (Wu et al., 2006; AMAP/UNEP, 2013). There have been few studies on anthropogenic GEM emissions in South Asia, the Indochinese Peninsula, and Central Asia. A previous study suggested that total Hg emission in India was about 253 t in 2004 (Mukherjee et al., 2009). Assuming GEM accounting for 64 % of total Hg emissions in India (Pacyna et al., 2003), GEM emission in India for 2004 was estimated to be 162 t, ∼ 2 times greater compared to the estimate of 96 t in South Asia (including India and other South Asian countries) for 2010 by the UNEP report (AMAP/UNEP, 2013). Given the increasing energy consumption recently, an increase in GEM emissions in South Asia is expected. This indicates that the UNEP report for 2010 may have underestimated GEM emissions in South Asia significantly.

Emission and re-emission of GEM from natural sources were regarded as an important cause of the discrepancy between estimated GEM emissions using correlation slopes of atmospheric pollutants and anthropogenic emission inventories (Jaffe et al., 2005; Slemr et al., 2006). Figure 7 shows the statistical summary of GEM exchange fluxes between different landscapes and the atmosphere in the warm season (from May to October) in mainland China. The mean GEM flux from dry farmland, rice paddies, grassland, forest soil, lake and river waters, and urban soil in warm seasons were $33.6 \pm 34.6$, $17.4 \pm 15.9$, $11.4 \pm 11.1$, $8.8 \pm 6.4$, $6.1 \pm 4.4$, and $35.3 \pm 43.1\,\mathrm{ng\,m^{-2}\,h^{-1}}$, respectively. These are significantly higher compared to those observed from Europe and North America (Poissant and Casimir, 1998; Boudala et al., 2000; Schroeder et al., 2005; Ericksen et al., 2006; Kuiken et al., 2008; Choi and Holsen, 2009). GEM fluxes from different landscapes in cold seasons (from November to April) were relatively limited. Several studies found that GEM

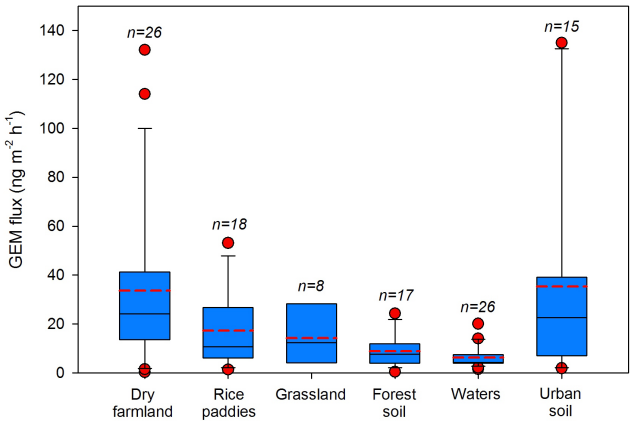


**Figure 7.** Statistical summary of GEM emission fluxes from typical landscapes in China in warm seasons (from May to October). The solid lines within each box represent the median fluxes, the dashed lines represent the mean, boundaries of the boxes represent 25th and 75th percentiles, whiskers indicate 10th and 90th percentiles, and red circles indicate fluxes < 10th percentile or > 90th percentile. References: Wang et al. (2003, 2006), Feng et al. (2004, 2005), Fang et al. (2004), Fu et al. (2007, 2008, 2010b, 2012c, 2013), Zhu et al. (2011, 2013), Ma et al. (2013), and Liu et al. (2014)

fluxes from dry farmland, forest soil, and lake waters were about 2.5–40 times (mean = 6.5, $n = 18$) lower than those in warm seasons (Wang et al., 2003; Ma et al., 2013; Fu et al., 2010b; Fu et al., 2013). Given the different landscapes and seasonal patterns of GEM fluxes in mainland China, we estimate the annual natural GEM emissions to be 528 t in China. This value is close to the estimate made by Shetty et al. (2008) but highlights the GEM emissions from dry farmland and grassland. There is no information regarding GEM fluxes from different landscapes in South Asia, the Indochinese Peninsula, and Central Asia. Here we assume that the natural GEM fluxes from landscapes in these areas are similar to those in China and the annual GEM emissions from South Asia, the Indochinese Peninsula, and Central Asia could be roughly estimated to be 240, 113, and 220 t, respectively.

Uncertainties and limitations related to the correlation slope method may also be important for the discrepancy between estimated GEM emissions and anthropogenic emission inventories. These uncertainties and limitations may include the uncertainties of CO, $CO_2$, and $CH_4$ emissions as well as the limitations of observed correlation slopes. The uncertainties for $CO_2$ and CO emissions in China in Table 3 were estimated to be about 11 and 45 %, respectively (Zhao et al., 2012a, b). Uncertainties for Chinese $CH_4$ emissions were not calculated by Zhang and Chen (2010) but are expected to have much larger values (Kurokawa et al., 2013). The uncertainties for $CO_2$, CO, and $CH_4$ emissions in South Asia, the Indochinese Peninsula, and Central Asia in Table 3 were estimated to be 44–49, 114–131, and 154–204 %, re-

spectively (Kurokawa et al., 2013). The limitations related to the correlation slopes were mainly caused by the fact that some of the emissions sources and pollution control devices of GEM, $CO_2$, CO, and $CH_4$ are different, and this is a particular issue for GEM / $CH_4$ correlation slopes. It possibly resulted in temporal and spatial variations of emission ratios between GEM and $CO_2$, CO, and $CH_4$. As shown in Sects. 3.2 and 3.3, GEM / CO and GEM / $CH_4$ correlation slopes for mainland China observed at WLG (mainly related to air masses from northern and northwestern China) were 66 and 145 %, respectively, higher than that observed at XGL and MAL (mainly related to air masses from southern and southwestern China), and this may reflect the spatial variations of correlation slopes in China. A seasonally dependent variation in GEM / CO correlation slopes in the upper troposphere of China was also observed (Slemr et al., 2009). It is speculated that the temporal and spatial variations of GEM / CO and GEM / $CO_2$ correlation slopes might be smaller than that of GEM / $CH_4$, mainly due to the fact that GEM, CO, and $CO_2$ have many common emission sources. Nevertheless, since the correlation slopes were not obtained uniformly within different seasons and regions of the studied regions, they may be important causes of the uncertainties and limitations of the correlation slope method. Therefore, more field observations are still needed in future to better constrain Hg emissions in Asia.

## 4 Conclusions

The correlation slopes of GEM / CO, GEM / $CO_2$, and GEM / $CH_4$ were calculated and applied for estimating the GEM emission from four important source regions in Asia using ground-based measurements at three remote sites in northwestern and southwestern China and backwards trajectory analysis. The values of GEM / CO, GEM / $CO_2$, and GEM / $CH_4$ correlation slopes varied by source region. The GEM / CO correlation slopes were comparable among mainland China, South Asia, and the Indochinese Peninsula, with the geometric means in the range of 7.3–7.8 $pg\,m^{-3}\,ppb^{-1}$, but they are about 2-fold lower than that in Central Asia (mean $= 13.4 \pm 9.5\,pg\,m^{-3}\,ppb^{-1}$). This is consistent with GEM / $CO_2$ correlation slopes for Central Asia (mean $= 315\,pg\,m^{-3}\,ppm^{-1}$), South Asia (mean $= 270\,pg\,m^{-3}\,ppm^{-1}$), and mainland China (mean $= 248\,pg\,m^{-3}\,ppm^{-1}$). However, we observed an opposite spatial trend for GEM / $CH_4$ correlation slopes that showed the highest geometric mean of $33.3 \pm 30.4\,pg\,m^{-3}\,ppb^{-1}$ in mainland China, followed by South Asia (mean $= 27.4 \pm 31.0\,pg\,m^{-3}\,ppb^{-1}$), the Indochinese Peninsula (mean $= 23.5 \pm 15.3\,pg\,m^{-3}\,ppb^{-1}$), and Central Asia (mean $= 20.5 \pm 10.0\,pg\,m^{-3}\,ppb^{-1}$). Elevated GEM / CO and GEM / $CO_2$ correlation slopes in Central Asia were found to be consistent with anthropogenic emission ratios of GEM relative to CO and $CO_2$, indicating anthropogenic sources played an important role in the observed correlation slopes. The highest GEM / $CH_4$ correlation slopes in mainland China were likely due to transport from northwestern China, where strong GEM emissions and weak $CH_4$ emissions occur.

The observed GEM / CO, GEM / $CO_2$, and GEM / $CH_4$ correlation slopes in Asia regions were consistently higher than those reported for Europe, North America, and South Africa. This highlights GEM emissions from non-ferrous smelting, mercury mining, natural sources, and historically deposited mercury (re-emission) in Asia. Using the correlation slopes of GEM / CO, GEM / $CO_2$ and recent inventories of CO and $CO_2$ in Asia countries, GEM emissions in mainland China, South Asia, the Indochinese Peninsula, and Central Asia were estimated to be in the ranges of 1071–1181, 340–470, 125, and 54–90 t, respectively. These estimates were lower than those predicted by the GEM / $CH_4$ correlation slopes because of the large uncertainties of $CH_4$ emissions in Asia as well as insufficient observations of GEM / $CH_4$ correlation slopes. These factors may lead to overestimation of GEM emissions. On the other hand, the estimates of GEM emissions in this study were much higher than those from recent anthropogenic GEM emission inventories. This discrepancy could be the result of underestimation of anthropogenic GEM emissions in Asia and GEM emissions from natural sources (including primary natural sources and re-emission of historically deposited mercury), and the uncertainties related to CO, $CO_2$, and $CH_4$ emissions and the limitations of observed correlation slopes. Our preliminary assessment showed an annual GEM emission of about 528 t from natural sources in mainland China, and 113–240 t for South Asia, the Indochinese Peninsula, and Central Asia. Although large uncertainties exist, these estimates seem to explain the discrepancies between the calculated GEM emissions based on the observed correlation slopes and anthropogenic emissions of GEM.

*Acknowledgements.* This work was funded by the National "973" Program of China (2013CB430003, 2010CB950601), the National Science Foundation of China (41273145, 41473025, 41003051, 41175116), the Innovative Program (Special Foundation for Young Scientist) of the Chinese Academy of Sciences (KZCX2-EW-QN111), and the European Commission through GMOS (project no. 265113). We also acknowledge J. Pacyna and the anonymous reviewer for their valuable suggestions on our original version of the article.

Edited by: R. Ebinghaus

## References


AMAP/UNEP: Technical Background Report for the Global Mercury Assessment 2013, Arctic Monitoring and Assessment Programme, Oslo, Norway/UNEP Chemicals Branch, Geneva, Switzerland., vi + 263 pp., 2013.

Boudala, F. S., Folkins, I., Beauchamp, S., Tordon, R., Neima, J., and Johnson, B.: Mercury flux measurements over air and water in Kejimkujik National Park, Nova Scotia, Water Air Soil Poll., 122, 183–202, doi:10.1023/A:1005299411107, 2000.

Brunke, E. G., Labuschagne, C., and Slemr, F.: Gaseous mercury emissions from a fire in the Cape Peninsula, South Africa, during January 2000, Geophys. Res. Lett., 28, 1483–1486, doi:10.1029/2000gl012193, 2001.

Brunke, E.-G., Ebinghaus, R., Kock, H. H., Labuschagne, C., and Slemr, F.: Emissions of mercury in southern Africa derived from long-term observations at Cape Point, South Africa, Atmos. Chem. Phys., 12, 7465–7474, doi:10.5194/acp-12-7465-2012, 2012.

Chen, H., Zhu, Q. A., Peng, C. H., Wu, N., Wang, Y. F., Fang, X. Q., Jiang, H., Xiang, W. H., Chang, J., Deng, X. W., and Yu, G. R.: Methane emissions from rice paddies natural wetlands, lakes in China: synthesis new estimate, Glob. Change Biol., 19, 19–32, doi:10.1111/Gcb.12034, 2013.

Cheng, Y. P., Wang, L., and Zhang, X. L.: Environmental impact of coal mine methane emissions and responding strategies in China, Int. J. Greenh. Gas. Con., 5, 157–166, doi:10.1016/j.ijggc.2010.07.007, 2011.

Choi, E. M., Kim, S. H., Holsen, T. M., and Yi, S. M.: Total gaseous concentrations in mercury in Seoul, Korea: local sources compared to long-range transport from China and Japan, Environ. Pollut., 157, 816–822, doi:10.1016/j.envpol.2008.11.023, 2009.

Choi, H. D. and Holsen, T. M.: Gaseous mercury fluxes from the forest floor of the Adirondacks, Environ. Pollut., 157, 592–600, doi:10.1016/j.envpol.2008.08.020, 2009.

Cole, A. S., Steffen, A., Pfaffhuber, K. A., Berg, T., Pilote, M., Poissant, L., Tordon, R., and Hung, H.: Ten-year trends of atmospheric mercury in the high Arctic compared to Canadian sub-Arctic and mid-latitude sites, Atmos. Chem. Phys., 13, 1535–1545, doi:10.5194/acp-13-1535-2013, 2013.

Ebinghaus, R., Jennings, S. G., Schroeder, W. H., Berg, T., Donaghy, T., Guentzel, J., Kenny, C., Kock, H. H., Kvietkus, K., Landing, W., Muhleck, T., Munthe, J., Prestbo, E. M., Schneeberger, D., Slemr, F., Sommar, J., Urba, A., Wallschlager, D., and Xiao, Z.: International field intercomparison measurements of atmospheric mercury species at Mace Head, Ireland, Atmos. Environ., 33, 3063–3073, doi:10.1016/S1352-2310(98)00119-8, 1999.

Ebinghaus, R., Slemr, F., Brenninkmeijer, C. A. M., van Velthoven, P., Zahn, A., Hermann, M., O'Sullivan, D. A., and Oram, D. E.: Emissions of gaseous mercury from biomass burning in South America in 2005 observed during CARIBIC flights, Geophys. Res. Lett., 34, L08813, doi:10.1029/2006gl028866, 2007.

EC-JRC/PBL: European Commission, Joint Research Center/Netherlands Environmental Assessment Agency, Emission Database for Global Atmospheric Research (EDGAR), release version 4.2, available at: http://edgar.jrc.ec.europa.eu/index.php (last access: 4 October 2012), 2011.

Ericksen, J. A., Gustin, M. S., Xin, M., Weisberg, P. J., and Fernandez, G. C. J.: Air-soil exchange of mercury from background soils in the United States, Sci. Total Environ., 366, 851–863, doi:10.1016/j.scitotenv.2005.08.019, 2006.

Fang, F. M., Wang, Q. C., and Li, J. F.: Urban environmental mercury in Changchun, a metropolitan city in Northeastern China: source, cycle, and fate, Sci. Total Environ., 330, 159–170, doi:10.1016/j.scitotenv.2004.04.006, 2004.

Fang, S. X., Zhou, L. X., Masarie, K. A., Xu, L., and Rella, C. W.: Study of atmospheric $CH_4$ mole fractions at three WMO/GAW stations in China, J. Geophys. Res.-Atmos., 118, 4874–4886, doi:10.1002/Jgrd.50284, 2013.

Feng, X. B., Yan, H. Y., Wang, S. F., Qiu, G. L., Tang, S. L., Shang, L. H., Dai, Q. J., and Hou, Y. M.: Seasonal variation of gaseous mercury exchange rate between air and water surface over Baihua reservoir, Guizhou, China, Atmos. Environ., 38, 4721–4732, doi:10.1016/j.atmosenv.2004.05.023, 2004.

Feng, X. B., Wang, S. F., Qiu, G. A., Hou, Y. M., and Tang, S. L.: Total gaseous mercury emissions from soil in Guiyang, Guizhou, China, J. Geophys. Res.-Atmos., 110, D14306, doi:10.1029/2004jd005643, 2005.

Friedli, H. R., Radke, L. F., Prescott, R., Hobbs, P. V., and Sinha, P.: Mercury emissions from the August 2001 wildfires in Washington State and an agricultural waste fire in Oregon and atmospheric mercury budget estimates, Global Biogeochem. Cy., 17, 1039, doi:10.1029/2002gb001972, 2003.

Friedli, H. R., Radke, L. F., Prescott, R., Li, P., Woo, J. H., and Carmichael, G. R.: Mercury in the atmosphere around Japan, Korea, and China as observed during the 2001 ACE-Asia field campaign: Measurements, distributions, sources, and implications, J. Geophys. Res.-Atmos., 109, D19s25, doi:10.1029/2003jd004244, 2004.

Fu, X. W., Feng, X. B., Wang, S. F., Qiu, G. L., and Li, P.: Mercury flux rate of to type s of grasslands in Guiyang, Research of Environmental Sciences, 20, 33–37, 2007 (in Chinese with abstract in English).

Fu, X. W., Feng, X. B., and Wang, S. F.: Exchange fluxes of Hg between surfaces and atmosphere in the eastern flank of Mount Gongga, Sichuan province, southwestern China, J. Geophys. Res.-Atmos., 113, D20306, doi:10.1029/2008jd009814, 2008.

Fu, X. W., Feng, X., Dong, Z. Q., Yin, R. S., Wang, J. X., Yang, Z. R., and Zhang, H.: Atmospheric gaseous elemental mercury (GEM) concentrations and mercury depositions at a high-altitude mountain peak in south China, Atmos. Chem. Phys., 10, 2425–2437, doi:10.5194/acp-10-2425-2010, 2010a.

Fu, X. W., Feng, X. B., Wan, Q., Meng, B., Yan, H. Y., and Guo, Y. N.: Probing Hg evasion from surface waters of two Chinese hyper/meso-eutrophic reservoirs, Sci. Total Environ., 408, 5887–5896, doi:10.1016/j.scitotenv.2010.08.001, 2010b.

Fu, X. W., Feng, X., Liang, P., Deliger, Zhang, H., Ji, J., and Liu, P.: Temporal trend and sources of speciated atmospheric mercury at Waliguan GAW station, Northwestern China, Atmos. Chem. Phys., 12, 1951–1964, doi:10.5194/acp-12-1951-2012, 2012a.

Fu, X. W., Feng, X., Shang, L. H., Wang, S. F., and Zhang, H.: Two years of measurements of atmospheric total gaseous mercury (TGM) at a remote site in Mt. Changbai area, Northeastern China, Atmos. Chem. Phys., 12, 4215–4226, doi:10.5194/acp-12-4215-2012, 2012b.

Fu, X. W., Feng, X. B., Zhang, H., Yu, B., and Chen, L. G.: Mercury emissions from natural surfaces highly impacted by human activities in Guangzhou province, South China, Atmos. Environ., 54, 185–193, doi:10.1016/j.atmosenv.2012.02.008, 2012c.

Fu, X. W., Feng, X. B., Guo, Y. N., Meng, B., Yin, R. S., and Yao, H.: Distribution and production of reactive mercury and dissolved gaseous mercury in surface waters and water/air mercury flux in reservoirs on Wujiang River, Southwest China, J. Geophys. Res.-Atmos., 118, 3905–3917, doi:10.1002/Jgrd.50384, 2013.

Gustin, M. S.: Are mercury emissions from geologic sources significant? A status report, Sci. Total Environ., 304, 153–167, Pii S0048-9697(02)00565-X, doi:10.1016/S0048-9697(02)00565-X, 2003.

Gustin, M. S., Lindberg, S., Marsik, F., Casimir, A., Ebinghaus, R., Edwards, G., Hubble-Fitzgerald, C., Kemp, R., Kock, H., Leonard, T., London, J., Majewski, M., Montecinos, C., Owens, J., Pilote, M., Poissant, L., Rasmussen, P., Schaedlich, F., Schneeberger, D., Schroeder, W., Sommar, J., Turner, R., Vette, A., Wallschlaeger, D., Xiao, Z., and Zhang, H.: Nevada STORMS project: Measurement of mercury emissions from naturally enriched surfaces, J. Geophys. Res.-Atmos., 104, 21831–21844, doi:10.1029/1999jd900351, 1999.

Gustin, M. S., Lindberg, S. E., Austin, K., Coolbaugh, M., Vette, A., and Zhang, H.: Assessing the contribution of natural sources to regional atmospheric mercury budgets, Sci. Total Environ., 259, 61–71, doi:10.1016/S0048-9697(00)00556-8, 2000.

Gustin, M. S., Engle, M., Ericksen, J., Xin, M., Krabbenhoft, D., Lindberg, S., Olund, S., and Rytuba, J.: New insights into mercury exchange between air and substrate, Geochim. Cosmochim. Ac., 69, A700–A700, 2005.

Huang, X., Li, M. M., Friedli, H. R., Song, Y., Chang, D., and Zhu, L.: Mercury Emissions from Biomass Burning in China, Environ. Sci. Technol., 45, 9442–9448, doi:10.1021/Es202224e, 2011.

Jaffe, D., Prestbo, E., Swartzendruber, P., Weiss-Penzias, P., Kato, S., Takami, A., Hatakeyama, S., and Kajii, Y.: Export of atmospheric mercury from Asia, Atmos. Environ., 39, 3029–3038, doi:10.1016/j.atmosenv.2005.01.030, 2005.

Kuiken, T., Zhang, H., Gustin, M., and Lindberg, S.: Mercury emission from terrestrial background surfaces in the eastern USA. Part I: Air/surface exchange of mercury within a southeastern deciduous forest (Tennessee) over one year, Appl. Geochem., 23, 345–355, doi:10.1016/j.apgeocliem.2007.12.006, 2008.

Kurokawa, J., Ohara, T., Morikawa, T., Hanayama, S., Janssens-Maenhout, G., Fukui, T., Kawashima, K., and Akimoto, H.: Emissions of air pollutants and greenhouse gases over Asian regions during 2000–2008: Regional Emission inventory in ASia (REAS) version 2, Atmos. Chem. Phys., 13, 11019–11058, doi:10.5194/acp-13-11019-2013, 2013.

Lan, X., Talbot, R., Castro, M., Perry, K., and Luke, W.: Seasonal and diurnal variations of atmospheric mercury across the US determined from AMNet monitoring data, Atmos. Chem. Phys., 12, 10569–10582, doi:10.5194/acp-12-10569-2012, 2012.

Lee, X., Bullock, O. R., and Andres, R. J.: Anthropogenic emission of mercury to the atmosphere in the northeast United States, Geophys. Res. Lett., 28, 1231–1234, doi:10.1029/2000gl012274, 2001.

Li, G. H., Feng, X. B., Li, Z. G., Qiu, G. L., Shang, L. H., Liang, P., Wang, D. Y., and Yang, Y. K.: Mercury emission to atmosphere from primary Zn production in China, Sci. Total Environ., 408, 4607–4612, doi:10.1016/j.scitotenv.2010.06.059, 2010.

Li, P., Feng, X. B., Qiu, G. L., Shang, L. H., Wang, S. F., and Meng, B.: Atmospheric mercury emission from artisanal mercury mining in Guizhou Province, Southwestern China, Atmos. Environ., 43, 2247–2251, doi:10.1016/j.atmosenv.2009.01.050, 2009.

Liang, S., Xu, M., Liu, Z., Suh, S., and Zhang, T. Z.: Socioeconomic drivers of mercury emissions in China from 1992 to 2007, Environ. Sci. Technol., 47, 3234–3240, doi:10.1021/Es303728d, 2013.

Lindberg, S., Bullock, R., Ebinghaus, R., Engstrom, D., Feng, X. B., Fitzgerald, W., Pirrone, N., Prestbo, E., and Seigneur, C.: A synthesis of progress and uncertainties in attributing the sources of mercury in deposition, Ambio, 36, 19–32, 2007.

Lindberg, S. E., Hanson, P. J., Meyers, T. P., and Kim, K. H.: Air/surface exchange of mercury vapor over forests – the need for a reassessment of continental biogenic emissions, Atmos. Environ., 32, 895–908, doi:10.1016/S1352-2310(97)00173-8, 1998.

Liu, F., Cheng, H. X., Yang, K., Zhao, C. D., Liu, Y. H., Peng, M., and Li, K.: Characteristics and influencing factors of mercury exchange flux between soil and air in Guangzhou City, J. Geochem. Explor., 139, 115–121, doi:10.1016/j.gexplo.2013.09.005, 2014.

Liu, M., Wang, H., Wang, H., Oda, T., Zhao, Y., Yang, X., Zang, R., Zang, B., Bi, J., and Chen, J.: Refined estimate of China's $CO_2$ emissions in spatiotemporal distributions, Atmos. Chem. Phys., 13, 10873–10882, doi:10.5194/acp-13-10873-2013, 2013.

Lou, Y. S., Li, Z. P., Zhang, T. L., and Liang, Y. C.: $CO_2$ emissions from subtropical arable soils of China, Soil Biol. Biochem., 36, 1835–1842, doi:10.1016/j.soilbio.2004.05.006, 2004.

Ma, M., Wang, D. Y., Sun, R. G., Shen, Y. Y., and Huang, L. X.: Gaseous mercury emissions from subtropical forested and open field soils in a national nature reserve, southwest China, Atmos. Environ., 64, 116–123, doi:10.1016/j.atmosenv.2012.09.038, 2013.

Mason, R. P., Fitzgerald, W. F., and Morel, F. M. M.: The biogeochemical cycling of elemental mercury – anthropogenic influences, Geochim. Cosmochim. Ac., 58, 3191–3198, doi:10.1016/0016-7037(94)90046-9, 1994.

Mukherjee, A. B., Bhattacharya, P., Sarkar, A., and Zevenhoven, R.: Mercury Emissions from Industrial Sources in India and its Effects in the Environment, Springer, New York, USA, 81–112, 2009.

Muntean, M., Janssens-Maenhout, G., Song, S. J., Selin, N. E., Olivier, J. G. J., Guizzardi, D., Maas, R., and Dentener, F.: Trend analysis from 1970 to 2008 and model evaluation of EDGARv4 global gridded anthropogenic mercury emissions, Sci. Tot. Environ., 494, 337–350, doi:10.1016/j.scitotenv.2014.06.014, 2014.

Munthe, J., Wangberg, I., Pirrone, N., Iverfeldt, A., Ferrara, R., Ebinghaus, R., Feng, X., Gardfeldt, K., Keeler, G., Lanzillotta, E., Lindberg, S. E., Lu, J., Mamane, Y., Prestbo, E., Schmolke, S., Schroeder, W. H., Sommar, J., Sprovieri, F., Stevens, R. K., Stratton, W., Tuncel, G., and Urba, A.: Intercomparison of methods for sampling and analysis of atmospheric mercury species, Atmos. Environ., 35, 3007–3017, doi:10.1016/S1352-2310(01)00104-2, 2001.

Munthe, J., Wangberg, I., Iverfeldt, A., Lindqvist, O., Stromberg, D., Sommar, J., Gardfeldt, K., Petersen, G., Ebinghaus, R., Prestbo, E., Larjava, K., and Siemens, V.: Distribution of atmospheric mercury species in Northern Europe: final results from the MOE project, Atmos. Environ., 37, S9–S20, doi:10.1016/S1352-2310(03)00235-8, 2003.

Nriagu, J. O.: A global assessment of natural sources of atmospheric trace-metals, Nature, 338, 47–49, doi:10.1038/338047a0, 1989.

Olivier, J. G. J., Berdowski, J. J. M., Peters, J. A. H., Bakker, J., Visschedijk, A. J. H., and Bloos, J. P. J.: Applications of EDGAR including a description of EDGAR 3.2: reference database with trend data for 1970–1995, RIVM, Bilthoven. RIVM report 773301001/NRP report 410 200 051., 2001.

Pacyna, E. G., Pacyna, J. M., Sundseth, K., Munthe, J., Kindbom, K., Wilson, S., Steenhuisen, F., and Maxson, P.: Global emission of mercury to the atmosphere from anthropogenic sources in 2005 and projections to 2020, Atmos. Environ., 44, 2487–2499, doi:10.1016/j.atmosenv.2009.06.009, 2010.

Pacyna, J. M., Pacyna, E. G., Steenhuisen, F., and Wilson, S.: Mapping 1995 global anthropogenic emissions of mercury, Atmos. Environ., 37, S109–S117, doi:10.1016/S1352-2310(03)00239-5, 2003.

Pan, L., Woo, J. H., Carmichael, G. R., Tang, Y. H., Friedli, H. R., and Radke, L. F.: Regional distribution and emissions of mercury in east Asia: a modeling analysis of Asian Pacific Regional Aerosol Characterization Experiment (ACE-Asia) observations, J. Geophys. Res.-Atmos., 111, D07109, doi:10.1029/2005jd006381, 2006.

Pirrone, N., Keeler, G. J., and Nriagu, J. O.: Regional differences in worldwide emissions of mercury to the atmosphere, Atmos. Environ., 30, 2981–2987, doi:10.1016/1352-2310(95)00498-X, 1996.

Pirrone, N., Cinnirella, S., Feng, X., Finkelman, R. B., Friedli, H. R., Leaner, J., Mason, R., Mukherjee, A. B., Stracher, G. B., Streets, D. G., and Telmer, K.: Global mercury emissions to the atmosphere from anthropogenic and natural sources, Atmos. Chem. Phys., 10, 5951–5964, doi:10.5194/acp-10-5951-2010, 2010.

Poissant, L. and Casimir, A.: Water-air and soil-air exchange rate of total gaseous mercury measured at background sites, Atmos. Environ., 32, 883–893, doi:10.1016/S1352-2310(97)00132-5, 1998.

Schroeder, W. H., Beauchamp, S., Edwards, G., Poissant, L., Rasmussen, P., Tordon, R., Dias, G., Kemp, J., Van Heyst, B., and Banic, C. M.: Gaseous mercury emissions from natural sources in Canadian landscapes, J. Geophys. Res.-Atmos., 110, D18302, doi:10.1029/2004jd005699, 2005.

Selin, N. E., Jacob, D. J., Park, R. J., Yantosca, R. M., Strode, S., Jaegle, L., and Jaffe, D.: Chemical cycling and deposition of atmospheric mercury: global constraints from observations, J. Geophys. Res.-Atmos., 112, D02308, doi:10.1029/2006jd007450, 2007.

Shetty, S. K., Lin, C. J., Streets, D. G., and Jang, C.: Model estimate of mercury emission from natural sources in East Asia, Atmos. Environ., 42, 8674–8685, doi:10.1016/j.atmosenv.2008.08.026, 2008.

Sheu, G. R., Lin, N. H., Wang, J. L., Lee, C. T., Yang, C. F. O., and Wang, S. H.: Temporal distribution and potential sources of atmospheric mercury measured at a high-elevation background station in Taiwan, Atmos. Environ., 44, 2393–2400, doi:10.1016/j.atmosenv.2010.04.009, 2010.

Slemr, F., Ebinghaus, R., Simmonds, P. G., and Jennings, S. G.: European emissions of mercury derived from long-term observations at Mace Head, on the western Irish coast, Atmos. Environ., 40, 6966–6974, doi:10.1016/j.atmosenv.2006.06.013, 2006.

Slemr, F., Ebinghaus, R., Brenninkmeijer, C. A. M., Hermann, M., Kock, H. H., Martinsson, B. G., Schuck, T., Sprung, D., van Velthoven, P., Zahn, A., and Ziereis, H.: Gaseous mercury distribution in the upper troposphere and lower stratosphere observed onboard the CARIBIC passenger aircraft, Atmos. Chem. Phys., 9, 1957–1969, doi:10.5194/acp-9-1957-2009, 2009.

Slemr, F., Weigelt, A., Ebinghaus, R., Brenninkmeijer, C., Baker, A., Schuck, T., Rauthe-Schoch, A., Riede, H., Leedham, E., Hermann, M., van Velthoven, P., Oram, D., O'Sullivan, D., Dyroff, C., Zahn, A., and Ziereis, H.: Mercury Plumes in the Global Upper Troposphere Observed during Flights with the CARIBIC Observatory from May 2005 until June 2013, Atmosphere-Basel, 5, 342–369, doi:10.3390/Atmos5020342, 2014.

Sprovieri, F., Pirrone, N., Ebinghaus, R., Kock, H., and Dommergue, A.: A review of worldwide atmospheric mercury measurements, Atmos. Chem. Phys., 10, 8245–8265, doi:10.5194/acp-10-8245-2010, 2010.

Streets, D. G., Hao, J. M., Wu, Y., Jiang, J. K., Chan, M., Tian, H. Z., and Feng, X. B.: Anthropogenic mercury emissions in China, Atmos. Environ., 39, 7789–7806, doi:10.1016/j.atmosenv.2005.08.029, 2005.

Streets, D. G., Zhang, Q., and Wu, Y.: Projections of global mercury emissions in 2050, Environ. Sci. Technol., 43, 2983–2988, doi:10.1021/Es802474j, 2009.

Tian, H. Z., Zhao, D., He, M. C., Wang, Y., and Cheng, K.: Temporal and spatial distribution of atmospheric antimony emission inventories from coal combustion in China, Environ. Pollut., 159, 1613–1619, doi:10.1016/j.envpol.2011.02.048, 2011.

Tohjima, Y., Kubo, M., Minejima, C., Mukai, H., Tanimoto, H., Ganshin, A., Maksyutov, S., Katsumata, K., Machida, T., and Kita, K.: Temporal changes in the emissions of $CH_4$ and CO from China estimated from $CH_4/CO_2$ and $CO/CO_2$ correlations observed at Hateruma Island, Atmos. Chem. Phys., 14, 1663–1677, doi:10.5194/acp-14-1663-2014, 2014.

Wang, D. Y., He, L., Shi, X. J., Wei, S. Q., and Feng, X. B.: Release flux of mercury from different environmental surfaces in Chongqing, China, Chemosphere, 64, 1845–1854, doi:10.1016/j.chemosphere.2006.01.054, 2006.

Wang, S., Feng, X., and Qiu, G.: The study of mercury exchange rate between air and soil surface in Hongfeng reservoir region, Guizhou, PR China, J. Phys. Iv., 107, 1357–1360, doi:10.1051/Jp4:20030553, 2003.

Wang, S. X., Zhang, L., Li, G. H., Wu, Y., Hao, J. M., Pirrone, N., Sprovieri, F., and Ancora, M. P.: Mercury emission and speciation of coal-fired power plants in China, Atmos. Chem. Phys., 10, 1183–1192, doi:10.5194/acp-10-1183-2010, 2010.

Wang, Y. Q., Zhang, X. Y., and Draxler, R. R.: TrajStat: GIS-based software that uses various trajectory statistical analysis methods to identify potential sources from long-term air pollution measurement data, Environ. Modell. Softw., 24, 938–939, doi:10.1016/j.envsoft.2009.01.004, 2009.

Weiss-Penzias, P., Jaffe, D., Swartzendruber, P., Hafner, W., Chand, D., and Prestbo, E.: Quantifying Asian and biomass

burning sources of mercury using the Hg/CO ratio in pollution plumes observed at the Mount Bachelor Observatory, Atmos. Environ., 41, 4366–4379, doi:10.1016/j.atmosenv.2007.01.058, 2007.

Worthy, D. E. J., Chan, E., Ishizawa, M., Chan, D., Poss, C., Dlugokencky, E. J., Maksyutov, S., and Levin, I.: Decreasing anthropogenic methane emissions in Europe and Siberia inferred from continuous carbon dioxide and methane observations at Alert, Canada, J. Geophys. Res.-Atmos., 114, D10301, doi:10.1029/2008jd011239, 2009.

Wu, Y., Wang, S. X., Streets, D. G., Hao, J. M., Chan, M., and Jiang, J. K.: Trends in anthropogenic mercury emissions in China from 1995 to 2003, Environ. Sci. Technol., 40, 5312–5318, doi:10.1021/Es060406x, 2006.

Yokouchi, Y., Taguchi, S., Saito, T., Tohjima, Y., Tanimoto, H., and Mukai, H.: High frequency measurements of HFCs at a remote site in east Asia and their implications for Chinese emissions, Geophys. Res. Lett., 33, L21814, doi:10.1029/2006gl026403, 2006.

Zhang, B. and Chen, G. Q.: Methane emissions by Chinese economy: inventory and embodiment analysis, Energ. Policy, 38, 4304–4316, doi:10.1016/j.enpol.2010.03.059, 2010.

Zhang, B., Li, J. S., and Peng, B. H.: Multi-regional input-output analysis for China's regional $CH_4$ emissions, Front Earth Sci.-Prc., 8, 163–180, doi:10.1007/s11707-014-0408-0, 2014a.

Zhang, H., Lindberg, S. E., Marsik, F. J., and Keeler, G. J.: Mercury air/surface exchange kinetics of background soils of the Tahquamenon River watershed in the Michigan Upper Peninsula, Water Air Soil Poll., 126, 151–169, doi:10.1023/A:1005227802306, 2001.

Zhang, H., Fu, X. W., Lin, C.-J., Wang, X., and Feng, X. B.: Observation and analysis of speciated atmospheric mercury in Shangrila, Tibetan Plateau, China, Atmos. Chem. Phys. Discuss., 14, 11041–11074, doi:10.5194/acpd-14-11041-2014, 2014b.

Zhang, L., Wang, S. X., Wang, L., and Hao, J. M.: Atmospheric mercury concentration and chemical speciation at a rural site in Beijing, China: implications of mercury emission sources, Atmos. Chem. Phys., 13, 10505–10516, doi:10.5194/acp-13-10505-2013, 2013.

Zhang, L. M., Wright, L. P., and Blanchard, P.: A review of current knowledge concerning dry deposition of atmospheric mercury, Atmos. Environ., 43, 5853–5864, doi:10.1016/j.atmosenv.2009.08.019, 2009.

Zhao, Y., Nielsen, C. P., and McElroy, M. B.: China's $CO_2$ emissions estimated from the bottom up: Recent trends, spatial distributions, and quantification of uncertainties, Atmos. Environ., 59, 214–223, doi:10.1016/j.atmosenv.2012.05.027, 2012a.

Zhao, Y., Nielsen, C. P., McElroy, M. B., Zhang, L., and Zhang, J.: CO emissions in China: uncertainties and implications of improved energy efficiency and emission control, Atmos. Environ., 49, 103–113, doi:10.1016/j.atmosenv.2011.12.015, 2012b.

Zhou, L. X., Tang, J., Wen, Y. P., Li, J. L., Yan, P., and Zhang, X. C.: The impact of local winds and long-range transport on the continuous carbon dioxide record at Mount Waliguan, China, Tellus B, 55, 145–158, doi:10.1034/j.1600-0889.2003.00064.x, 2003.

Zhu, J. S., Wang, D. Y., Liu, X. A., and Zhang, Y. T.: Mercury fluxes from air/surface interfaces in paddy field and dry land, Appl. Geochem., 26, 249–255, doi:10.1016/j.apgeochem.2010.11.025, 2011.

Zhu, J. S., Wang, D. Y., and Ma, M.: Mercury release flux and its influencing factors at the air–water interface in paddy field in Chongqing, China, Chinese Sci. Bull., 58, 266–274, doi:10.1007/s11434-012-5412-8, 2013.